

Modifications of Wind Response of Tall-Building Caused by Interfering Effects: A CFD Approach

E.M.R. Ekanayake, H.M.A.I. Herath, B. Kiriparan and J.A.S.C. Jayasinghe

Abstract: The wind is an essential factor to consider in the design and construction of tall buildings. As buildings get taller, the wind's impact becomes more significant, and the building's stability and safety become more critical. The interfering effect is one of the significant consequences of a building that needs to be considered. The "interfering effect" is a phenomenon in wind engineering that occurs when an upstream structure affects the wind load on a downstream building. In the past, most of the studies of interfering effects were done with 2D or 3D simulations, only considering one or two parameters from the shape, height, and angle. Therefore, this research attempts to analyze the interfering effect qualitatively and quantitatively from the upstream building to a selected square-shaped principal building by varying the height of the interfering building with different shapes, namely, circular, cross, and triangular shapes with different orientations based on 3D CFD modeling. The commercial CFD package Midas NFX is used for this numerical analysis. The results from the base moment and base shear suggest that a safety factor for interfering effects should be considered in designing the building structures in the city area to ensure the stability of the building, and it is, for the worst-case scenario, 1.3. The pressure fluctuation results highlighted the importance of designing the connection of the cladding system to both compression and tension forces. The findings of the present paper will be crucial in ensuring the stability and safety of the building structures when those buildings are in a dense building environment.

Keywords: CFD Simulation, Interfering effect, Turbulence model, Wind response, Wind tunnel test

1. Introduction

Due to global urbanization, high-rise buildings are becoming a more common characteristic in cities to meet human thoughts and needs within limited areas. The wind is a major factor in determining the lateral load on tall buildings. The impact of wind loads on buildings can manifest in various ways, such as interfering effects, dynamic response, wind-borne debris, and aerodynamic instabilities. Among these impacts, the interfering effect is a significant phenomenon that may alter the wind flow characteristics around the building due to the influence of adjacent buildings [1]. Based on the shape and orientation of the upstream building, the interfering effect changes the wind load [2].

Previous research on interfering effects mostly used 2D or 3D simulations and only took into account one or two parameters related to shape, height, and angle [3,4,5]. A few research have concentrated on the interference effects of the height change of the interfering building [6]. Therefore, this study uses 3D CFD modeling to principal building. Accurate prediction of wind behaviour around buildings is crucial for optimizing building design. The wind analysis can be conducted based on currently available

vary the height of the interfering building with various shapes, including circular, cross, and triangular shapes with different orientations, in order to analyze the interfering effect qualitatively and quantitatively from the upstream building to a chosen square-shaped

Eng. E.M.R. Ekanayake, Student Member of IESL, B.Sc. Eng. (Hons) (Peradeniya), Department of Civil Engineering, Faculty of Engineering, University of Peradeniya.

Email: ekanayakeravindra@gmail.com

ORCID ID: <https://orcid.org/0009-0008-4911-7679>

Eng. H.M.A.I. Herath, Student Member of IESL, B.Sc. Eng. (Hons) (Peradeniya), Department of Civil Engineering, Faculty of Engineering, University of Peradeniya.

Email: anjanaindunil97@gmail.com

ORCID ID: <https://orcid.org/0009-0003-6785-481X>

Eng. B. Kiriparan, C.Eng., MIE(SL), B.Sc. Eng. (Hons) (Peradeniya), Department of Civil Engineering, Faculty of Engineering, University of Peradeniya.

Email: kiriparan@gmail.com

ORCID ID: <https://orcid.org/0000-0003-4633-7234>

Eng. (Dr.) J.A.S.C. Jayasinghe, AMIE(SL), B.Sc. Eng. (Peradeniya), M.Eng. (AIT), Ph.D. (Tokyo), Senior Lecturer, Department of Civil Engineering, Faculty of Engineering, University of Peradeniya

Email: supunj@eng.pdn.ac.lk

ORCID ID: <http://orcid.org/0000-0003-1054-9358>



wind codes, computational fluid dynamics (CFD) simulations, and wind tunnel testing. Most wind codes have been unable to provide accurate results on high-rise buildings with irregular geometries and apply only to buildings less than 200 meters high and have a regular shape [7]. The other two methods, wind tunnel tests and Computational Fluid Dynamics (CFD), are frequently used to analyse tall buildings with irregular geometries as they have the flexibility to analyse any type of building. But the wind tunnel test method is expensive and time-consuming to set up and conduct tests. When considering the CFD simulation method, it gives adequately accurate results with limited resources. In this study, wind flows around the building are analysed by using Computational Fluid Dynamic (CFD) approach.

First, the CFD software was used to model the selected building structure from the literature [8]. There are three main approaches in CFD simulation for wind analysis: Reynolds-averaged Navier-Stokes equations (RANS equations), Large eddy simulation (LES), and Direct numerical simulation (DNS). According to the literature, DNS gives more accurate results but requires more computational power whereas RANS gives reasonably accurate results with less computational power. The RANS approach is utilized in this study to model the turbulent flow due to computer facility limitations. The findings were validated using published wind tunnel test results for the same building. The validated CFD model was used to identify the interference effect on a square-shaped principal building from the upstream building with different shapes, orientations, and heights. This study presents the comparison of the base moment, base shear, and pressure fluctuation of the principal building to assess the impact of the upstream building considering the interfering effects.

2. Wind-induced Responses of Tall Buildings

As urbanization progresses and building technologies advance, modern tall structures are becoming slender, more flexible, lightweight, and exhibit lower damping properties. However, this trend also makes them more susceptible to wind-induced dynamic excitations, increasing their vulnerability [9]. Tall building wind design typically considers along wind, across wind, and torsional responses, as illustrated in Figure 1. Wind design codes and standards are employed during the preliminary

design stages to estimate the impact of wind on tall buildings.

In-depth investigation and analysis of the responses and behaviours of individual buildings are critical in developing and optimizing building designs. Wind loads are particularly significant for tall buildings, especially in cyclone-prone areas, as these structures are prone to wind-induced vibrations due to increased flexibility and limited damping properties [10]. Wind is generated by the differential heating of the atmosphere by the sun, resulting in large-scale wind patterns driven by differences in solar energy absorption between the equator and the poles. Wind effects on structures can be categorized into static and dynamic effects [11]. Static effects result in elastic bending and twisting of the structure, while dynamic effects cause vibrations or oscillations. The wind is characterized by a constant mean wind velocity and varying gust velocity, resulting in both mean and fluctuating wind forces.

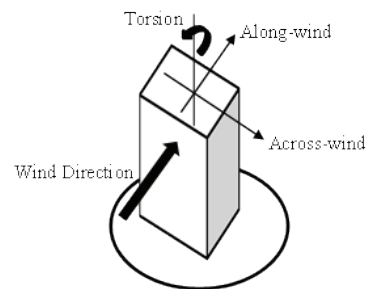


Figure 1 - Wind Responses of a Building

2.1 Along-Wind Response

The along-wind response of a building is primarily influenced by pressure variations on both the windward face (the frontal face exposed to the wind) and the leeward face (the back face) of the structure, as depicted in Figure 2. This response can be considered to have both a mean component caused by the mean wind speed, and a fluctuating component. The fluctuating component is caused by differences in wind speed from the mean and is typically composed of a random collection of eddies of various sizes [12]. The gust factor approach can provide reasonably accurate predictions of the dynamic response of buildings in the along-wind direction. The along-wind response of structures can be modeled as single- or multiple-degree-of-freedom systems [13].

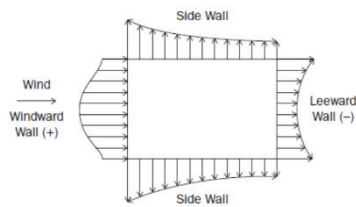


Figure 2 - Pressure Fluctuations of the Structure due to Wind Load [14]

2.2 Across-Wind Response

Across-wind response of a tall building refers to the vibration transverse to the wind direction. This response is often the result of vortex shedding and can cause significant discomfort for building occupants. The frequency of the across-wind response depends on the building's natural frequency and wind speed. In general, as the wind speed increases, the frequency of the across-wind response also increases. The severity of the across-wind response can be assessed by calculating the peak acceleration of the building. To mitigate the across-wind response, various techniques such as tuned mass dampers, aerodynamic modifications, and passive control systems have been employed. Proper design and assessment of the across-wind response of tall buildings are crucial for ensuring the safety and comfort of building occupants and preventing damage to the structure. To excite modern tall buildings and structures across-wind, there are three mechanisms and their higher time derivatives. These mechanisms include incident turbulence, vortex shedding, and higher derivatives of across-wind displacement [15].

2.3 Torsional Response

The impact of wind-induced forces on tall buildings can result in lateral movements and significant twisting, known as torsion. The torsional response is a crucial aspect of understanding the dynamic behavior of tall buildings under wind loads. Various factors, including the building's shape and orientation, wind speed and direction, and surrounding structures, can influence the torsional response. Various investigations have been conducted to examine the torsional response of tall buildings. These include computational studies that employed dynamic pressure and force data obtained from wind-tunnel models [16], as well as experimental investigations carried out on aero-elastic models with torsional degrees of freedom [17]. Cheung and Melbourne [18], Lythe and Surry [19], and Isyumov and Poole [20] conducted an investigation to explore whether torsional motions enhance the perception of

motion when assessing accelerations near the peripheral sections of a tall building. The outcomes of these studies have provided valuable insights into the dynamic behavior of tall buildings under wind loads, which can be useful in enhancing their design and construction to ensure their safety and stability in high wind conditions.

2.4 Interference Effects

The impact of the surrounding building on the wind loading of a building considered is known as the interference effect. According to wind tunnel research, interfering effects do not always lower wind loads on a given building and can instead increase wind loads, which can have negative implications. In the 1930s, research on the "Interference effect" began on the Empire State Building [21]. This topic has been the subject of ongoing research since then. Several investigations have demonstrated that assessing an isolated structure according to wind codes has rather adverse wind effects.

Interfering effects can arise from various factors, including the orientation, height, geometry, and wind direction of surrounding buildings in relation to the tall building. The presence of neighboring buildings can significantly influence the wind flow patterns and pressure distribution around the tall building, leading to changes in wind loads. These effects can be complex and vary depending on the specific location and configuration of the tall building and its surroundings. Firstly, the Interference Factor (IF) was introduced by Saunders and Melbourne [22] to measure the interfering effect. Figure 3 explains the interference effect of the upstream building.

$$\text{Interference Factor} = \frac{\text{Force on Building with interfering building present}}{\text{Force on Isolated building}}$$

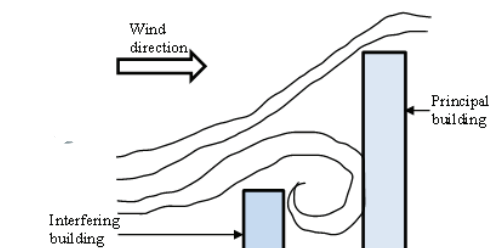


Figure 3 - Interfering Effect

3. Numerical Modeling of Fluid Flow Around a Building

The CFD approach is a technique used to solve the Navier-Stokes equations, which describes the motion of fluids in the numerical domain. The equations are solved in a numerical grid that represents the geometry of the building and the



surrounding fluid domain. CFD models are capable of simulating various fluid phenomena, such as turbulence, flow separation, and vortices. They can also provide detailed information about the flow field, such as velocity and pressure distribution, and can be used to predict the wind loads acting on the building.

3.1 Available Numerical Approaches

There are several numerical approaches available in CFD for wind analysis. Some of the commonly used approaches are, RANS, LES, and DNS. RANS approach averages the equations governing fluid flow over time [23], resulting in a time-averaged solution. It is commonly used for predicting mean wind loads on buildings [24]. The LES approach resolves the largest turbulent scales of motion and models the smallest ones [25]. It is commonly used for predicting wind loads on buildings with complex shapes. DNS is a CFD approach that solves Navier-Stokes equations directly without using any turbulence model. According to the literature, DNS gives more accurate results but requires more computational power. Besides, RANS gives reasonably accurate results with less computational power [23]. The RANS approach is utilized in this study to model the turbulent flow due to the available limited computer facility.

3.2 RANS Approach

The RANS approach is a widely used method for simulating fluid flows in CFD. In RANS, the governing equations for fluid flow are averaged over time, and the turbulent stresses are modeled using turbulence models. Various turbulence models based on the Reynolds Average Navier-Stokes Equations are:

- Zero equation model (Mixing length model)
- One equation model (Sapalart-Allmaras)
- Two equation models ($k-\epsilon$ models)
- Three equation model ($k-\epsilon-\phi$ by Kawamoto)
- Seven equation model (Reynolds stress model)

The selection of a turbulence model is based on factors such as computer resources, accuracy requirements, problem type, and simulation time, which are all relevant considerations in choosing an appropriate turbulence model for computational fluid dynamics (CFD) simulation [26]. The 2 - equation $k-\epsilon$ turbulence model is widely used in wind engineering problems because of its high reliability. Furthermore, in numerical simulation, 2 equation $k-\epsilon$, and

2 equation $k-\omega$ (SST) are recognized as better turbulence models because they forecast the net pressure distribution throughout the perimeter better than the other turbulence models [27].

3.3 CFD Simulation of Flow around a Building Structure by using Midas NFX

The Commonwealth Advisory Aeronautical Council (CAARC) standard tall building is being used as the pre-determined building to compare the reliability of turbulence models with experimental data. The selected prototype building is rectangular and prismatic, with dimensions of 100 ft x 150 ft (30.48 x 45.72 m) for its sides and a height of 600 ft (182.88 m) [8]. Figure 4 shows the shape and dimensions of the CAARC building.

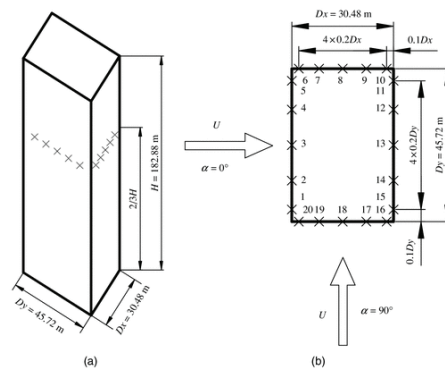


Figure 4 - Shape and Dimensions of CAARC Building [8]

Figure 5 shows the wind tunnel test data that five different institutions, namely the University of Bristol -England (Bristol), City University - England (City), Monash University-Australia (Monash), and National Aeronautical Establishment-Canada (a & b) (NAE) conducted on CAARC standard tall buildings [8].

In Figure 5, L is the perimeter of the principal building and X^* is the considered distance along the perimeter.

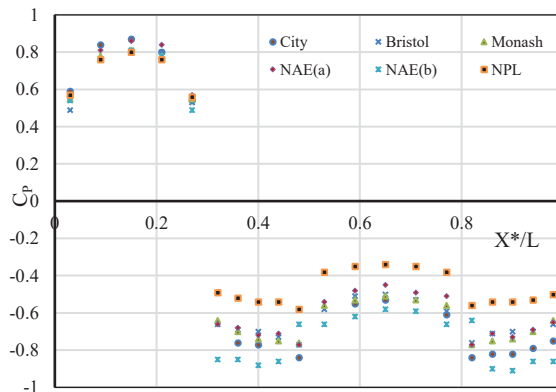


Figure 5 - Wind Tunnel Test Data of CAARC Building

3.3.1 Computational Domain

To prevent the computational domain of the surface from affecting the surface pressure over buildings, it is necessary to maintain a sufficient distance between the building surface and the computational boundary. To ensure accurate modeling of the flow around both low-rise and high-rise buildings, it is necessary to maintain a minimum length of 5 times the height of the building for the upstream and downstream zones [28]. In Computational Fluid Dynamics (CFD) simulations of tall buildings, several variables have been suggested and adopted. To achieve accurate simulations, it is typically advised to maintain a computational domain with a width and height that are 6 times and 2 - 2.5 times the building width and height, respectively. Additionally, the downstream and upstream zones should be of length approximately 2 - 2.5 times and 1 - 1.5 times the building height, respectively.

Figure 6 illustrates the development of the CAARC model on the Midas NFX platform, with a computational domain of 945 m × 855 m × 500 m (L × W × H). To ensure adequate space for wind development, the downstream and upstream distances were set at 732 m and 183 m, respectively. The computational setting must meet specific requirements to ensure that the numerical model closely resembles the real model and avoids blockage effects. The blockage ratio (δ) should not exceed 5%, and in this study, the blockage ratio was 1.89% as determined by Eq 1.

$$\delta = \frac{A}{A_0} \quad \dots(1)$$

The exponential wind profile was chosen to model the wind behavior around the CAARC standard tall building, which stands at a significant height within the atmospheric boundary layer. In wind tunnel studies, the velocity profile of the atmospheric boundary layer can be characterized by two laws: power law and log law. The power law describes a steeper variation in wind speed than the log law [29]. For this study, the power law given in Eq 2 was utilized.

$$\frac{U(Z)}{U_H} = \left(\frac{Z}{Z_H}\right)^\alpha \quad \dots(2)$$

Eq 2 defines $U(Z)$ as the wind speed at height Z , where Z_H is the building height of 180 m with a wind speed of 12.7 m/s as U_H . The wind profile coefficient, α , which is set at 0.3, is also taken into consideration in this equation.

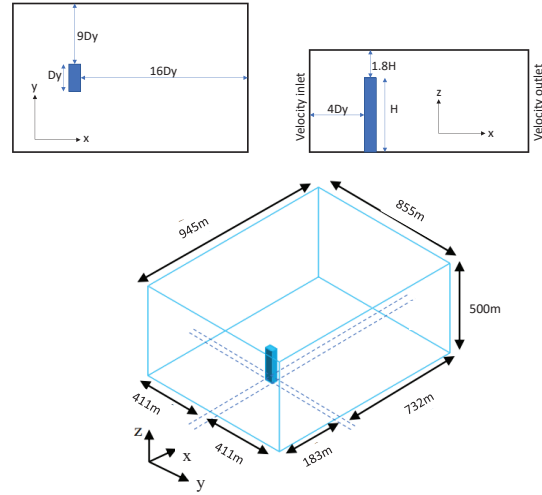


Figure 6 - Computational Domain of CFD Model

3.3.2 Boundary Conditions

The boundary conditions for the fluid domain were set as follows:

- The inlet face was specified along the x-axis with a given velocity profile function.
- The outlet face was set to zero pressure.
- The velocity component V_x was set to zero at the faces along the y-direction.
- The velocity component V_z was set to zero at the top surface of the computational domain.

A no-slip condition was applied to the bottom surface of the fluid domain, as well as where the building surfaces come into contact with the fluid domain [30, 31].

As shown in Figure 7, mesh was generated by setting the element size growth rate as 1.05 and ratio between minimum and maximum element size as 2, the density of air as 1.25 kg m⁻³, and the viscosity of air as 1.79x10⁻⁵ kg/m.s, turbulent intensity as 0.003.

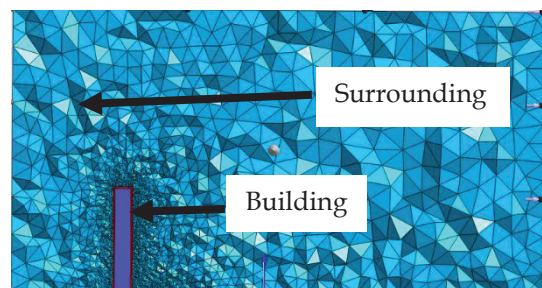


Figure 7 - Sectional View of CFD Domain

3.3.3 Sensitivity Analysis for Different Mesh Sizes

In order to ensure accurate numerical results, it is essential to choose an appropriate grid size prior to conducting simulations. To assess the



impact of grid resolution on wind pressure coefficients, both the grid size and the number of grids were adjusted. Four models were developed with varying degrees of grid resolution using the $2k - \epsilon$ model. The resulting wind pressure coefficients were computed using Eq. 3.

$$C_{pi} = \frac{P_i - P_\alpha}{\frac{1}{2}\rho U_\alpha^2} \quad \dots(3)$$

The wind pressure coefficient at a specific point i is given by Eq. 3, where C_{pi} is the mean wind pressure coefficient, P_i represents the wind pressure, P_α is the static pressure at the reference height, ρ is the air density, which is 1.25 kg m^{-3} in this study, and U_α is the wind speed at the reference height. At the top of the CAARC building located at 180 m [32,33], the wind speed is 12.7 m/s . The mean pressure coefficients on each surface at 2/3 height of the CAARC standard tall building are presented in Figure 8.

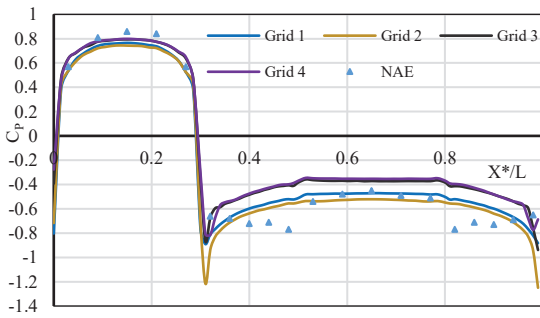


Figure 8 - Sensitivity Analysis of Different Grid Sizes for CAARC Standard Tall Building

To assess the accuracy of the results, the National Aeronautical Establishment-Canada (NAE-a) case was used for sensitivity analysis. To quantify the accuracy of the results, the mean absolute percentage error (MAPE), mean absolute deviation (MAD), and mean squared deviation (MSD) were calculated using Eqs. (4), (5) and (6), respectively [34].

$$MAPE = \frac{\sum_{t=1}^n \left| \frac{C_{pitunnel} - C_{piCFD}}{C_{pitunnel}} \right|}{n} \times 100\% \quad \dots(4)$$

$$MAD = \frac{\sum_{t=1}^n |C_{pitunnel} - C_{piCFD}|}{n} \quad \dots(5)$$

$$MSD = \frac{\sum_{t=1}^n |C_{pitunnel} - C_{piCFD}|^2}{n} \quad \dots(6)$$

Based on Table 1, it can be inferred that achieving a grid resolution of 0.5 m on the building surface would meet the necessary numerical accuracy standards.

Table 1 - Sensitivity of Wind Pressure Coefficients to Grid Resolution

Error	Grid 1 (0.5m)	Grid 2 (1.0m)	Grid 3 (1.5m)	Grid 4 (2.0m)
MAPE	13.42	14.97	23.24	25.85
MAD	0.09	0.10	0.15	0.17
MSD	0.01	0.017	0.03	0.04

3.4 Selection of the Most Reliable RANS Turbulence Model

The experimental data from wind tunnels were compared to each turbulent model independently. The distribution of C_{pi} obtained using different turbulence models; 0 equation model, 1 - equation $k - \epsilon$ model, 2-equation Standard $k - \epsilon$ model, 2 - equation $k - \omega$ model and 2 - equation $k - \omega$ SST model were compared with the experimental data. Table 2 shows three errors calculated using Eqs. (4), (5) and (6). According to those results, the 2 $k - \omega$ SST model shows minimum MAPD, MAD and MSD values. The comparison results for the above five turbulence models are shown in Figure 9.

Table 2 - Comparison between Numerical Results and Experimental Results

Error	0 eq	1 ke	2 ke	2 k - w	2 k - w sst
MAPE	14.10	15.01	14.97	19.40	11.88
MAD	0.08	0.10	0.10	0.13	0.07
MSD	0.01	0.01	0.02	0.03	0.01

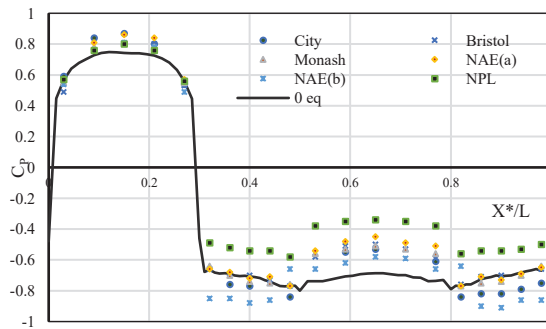


Figure 9(a)

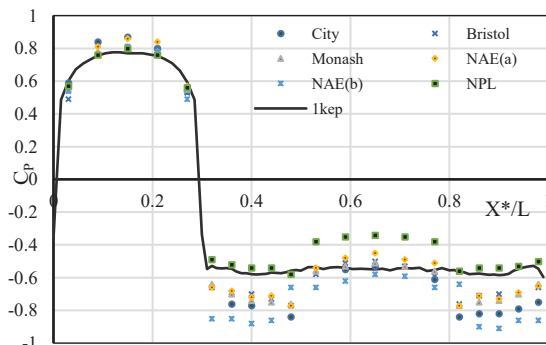


Figure 9(b)

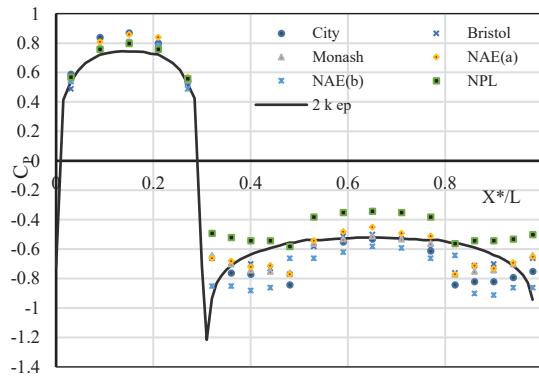


Figure 9(c)

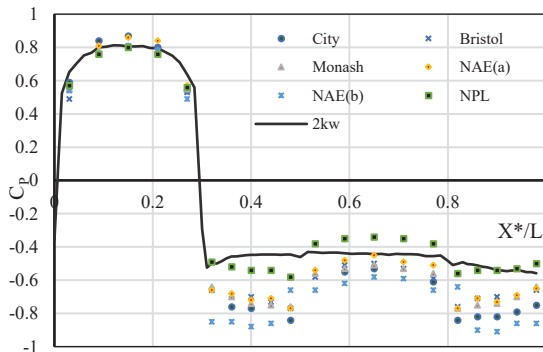


Figure 9(d)

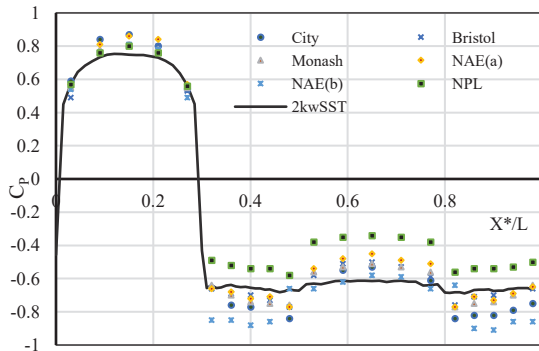


Figure 9(e)

Figure 9 - Pressure Variation of CAARC Building Model for Different Turbulence Models: (a) $0\epsilon q$ Model, (b) $1k - \epsilon$ Model, (c) $2k - \epsilon$ Model, (d) $2k - w$ Model and (e) $2k - w$ SST Model

4. Parametric Study

A parametric study was conducted to assess the impact of height, orientation, and shape of tall buildings on wind-induced response, including the interference effect, using computational fluid dynamics (CFD) and the following are some key aspects of the suggested methodology. *A* is the principal building and *B* is the interfering building. Based on the literature, buildings with square or rectangular plan shapes are known to

experience higher wind effects compared to other common plan shapes [35,36]. Therefore, for this study, building *A* has fixed geometries including length, width, and height of 24 m, 24 m and 150 m, respectively. The orientation ($\theta = 0^\circ, 45^\circ, 90^\circ$), height ($h = 50\text{ m}, 100\text{ m}, 150\text{ m}, 175\text{ m}$) and shape of building *B* will be changed while keeping the plan areas of the selected shapes remaining the same. As shown in Figure 10, building *A* is a fixed building, and the location of building *B* will be changed with the changing of the orientation. *X* is the length between building *A* and building *B*, and it has a fixed value of 25 m (Minimum separation distance between tall buildings on the same site of 25 m or greater) [37]. θ is the angle between the two buildings.

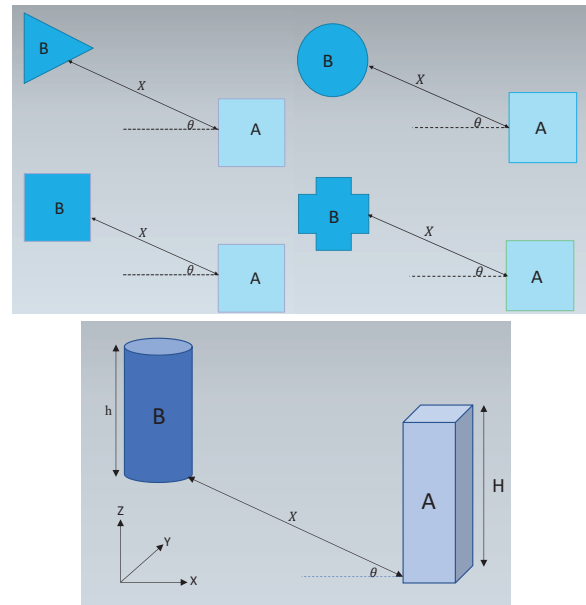


Figure 10 - Building Configuration for Parametric Study

For the parametric study, the mesh size was chosen as 0.5 m and the turbulence model as $2k - \omega$ SST, based on the previous analysis results. As shown in Figure 11, a total of 48 combinations were studied to identify their interfering effects. The responses (pressure distribution, interfering factor, base shear, and overturning moment) are compared in this study. First, the responses on the principal building were evaluated while keeping one angle and height unchanged for different plan shapes. From that, the critical shape which gives the highest interfering effect for that height and the angle was identified. Subsequently, the influence of angle was compared. Finally, using those results, the critical angle for the selected shape and the height was identified.



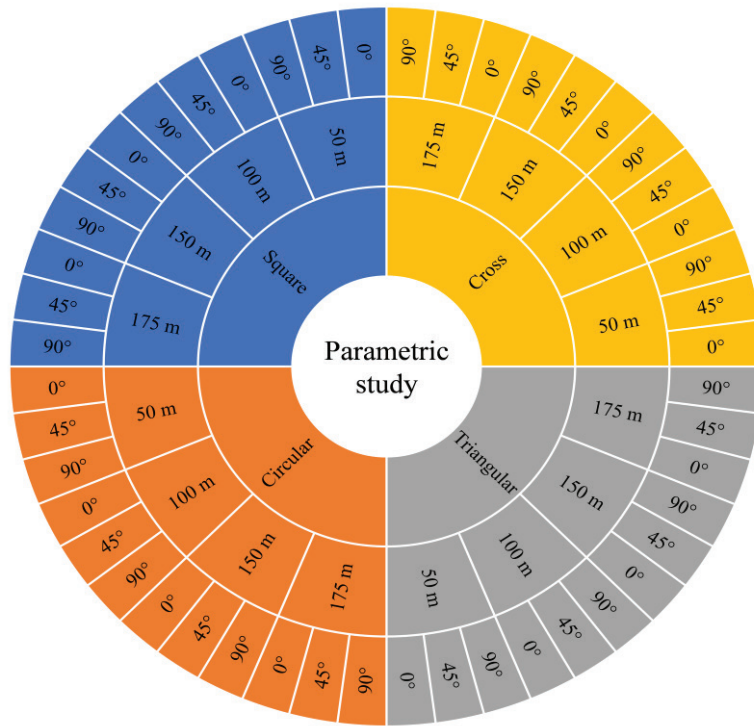


Figure 11 - All the Combinations of Parametric Study

4.1 Base Moment Comparison

The maximum deviation was obtained at the 0-degree 175 m case with the triangular shape. To represent that, the base moment values of the 0 degree and 175 m cases were compared for all shapes and the comparison is shown in Figure 12. Deviation was calculated based on Eq. (7). The results indicate that the triangular shape has the maximum deviation of 94.67%, while the square shape has the minimum deviation of 84.43%.

$$Deviation = \left| \frac{Isolated\ condition - |Interfering\ condition|}{Isolated\ condition} \right| \times 100\% \dots(7)$$

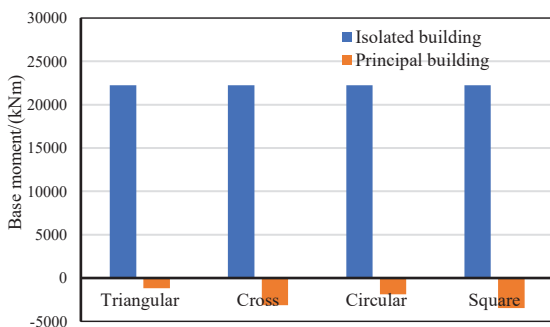


Figure 12 - Base Moment due to Wind Loading for 0-deg 175 m Case

Next, results were compared for the triangular shape case with different angles, as shown in Figure 13. In this case, the maximum deviation of 94.67% is shown in the 0-deg case and the minimum deviation of 32.38% is shown in 90-deg case.

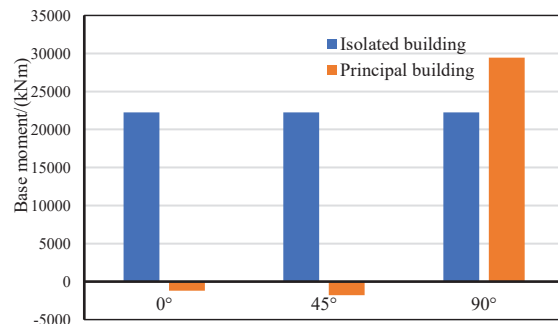


Figure 13 - Base Moment due to Wind Loading for 175 m Triangular Shape Case

4.2 Base Shear Comparison

The comparison of base shear for the 0-deg and 175 m cases for all shapes is shown in Figure 14. The results indicate that the circular shape has the maximum deviation of 99.62%, while the square shape has the minimum deviation of 88.38%.

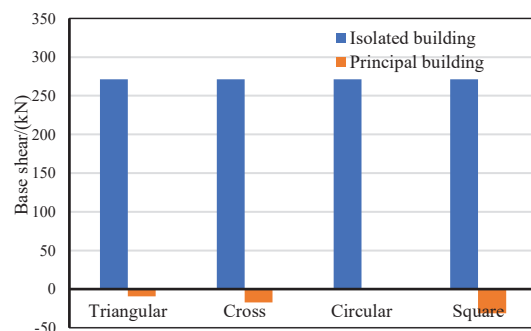


Figure 14 - Base Shear due to Wind Loading for 0-deg 175 m Case

Next, results were compared for the circular shape 175 m case with different angles, as shown in Figure 15. In that, the maximum deviation of 99.62% is shown in 0-deg case and the minimum deviation of 0.19% is shown in 45-deg case.

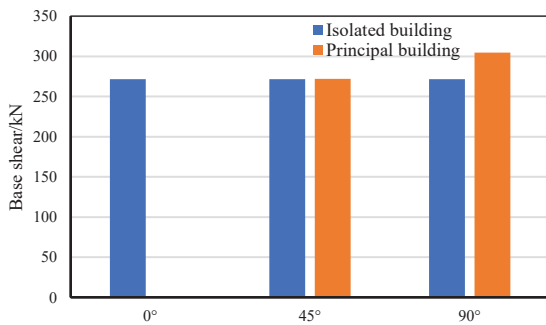


Figure 15 - Base Shear due to Wind Loading for 175 m Circular Shape Case

Similarly, the outcomes for all the other cases were compared. Results obtained are shown in Figures 16 and 17. According to base moment

results, a maximum deviation of 94.67% is shown in the triangular 0-deg 175 m case and a minimum deviation of 0.04% is shown in the circular 0-deg 50 m case.

According to base shear results, a maximum deviation of 99.62% is shown in circular 0-deg 175 m case and a minimum deviation of 0% is shown in circular 45-deg 50 m case. Also, increment was calculated based on Eq. (8).

$$Increment = \frac{Interfering\ condition - Isolated\ condition}{Isolated\ condition} \times 100\% > 0.. (8)$$

Based on the results, the maximum increments of the base moment and base shear in the triangular 90-deg and 175 m case were observed, and they were 32.38% and 31.30%, respectively. For all shapes at 0 degrees, the interfering effect initially increased with the height of the interfering building until it reached the height of the principal building. After that, the interfering effect decreased with further increases in the height of the interfering building.

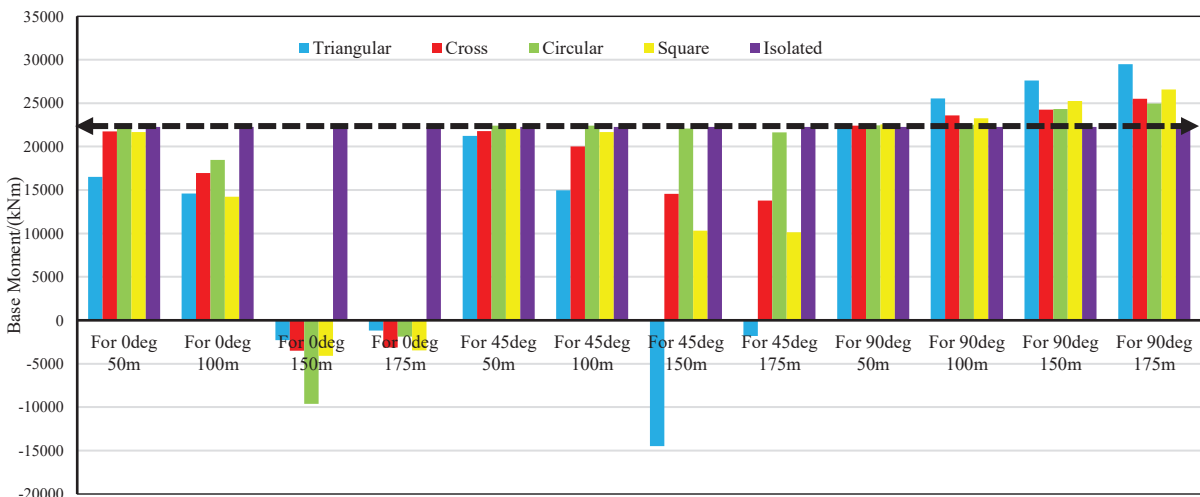


Figure 16 - Comparison of Base Moment due to Wind Loading for all Combinations

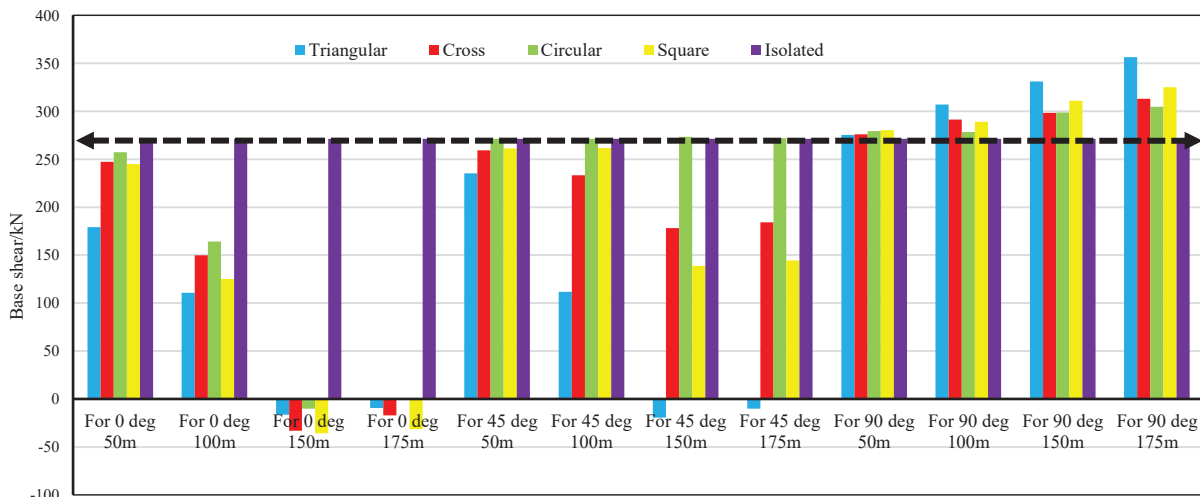


Figure 17 - Comparison of Base Shear Force due to Wind Loading for all Combinations



4.3 Pressure Variation Comparison

Next, this work extended to study the variation of the mean C_p along the height at the centerline of the windward face for each defined combination. Figure 18 shows the results of the analysis, which reveal that the presence of an interfering building causes a drastic variation in C_p along the height of the building for all shapes. Maximum variation is shown in triangular shape and minimum variation shown in circular shape.

As shown in Figure 19, the variation of C_p along the height of the interfering building differs significantly for different orientations in the case of a square shape with a height of 150 m.

The maximum variation is observed in the 0-deg orientation of the interfering building, while the

minimum variation is observed in the 90-deg orientation of the interfering building.

As shown in Figure 20, higher interfering buildings create larger negative pressure zones. The angle between buildings also impacts the pressure, with larger angles resulting in positive pressure on the windward face of the principal building.

As shown in Figure 21, the windward face is positive, and the leeward and sidewalls are negative for the isolated model. However, when considering 150 m square shape cases where a building interferes with the isolated model, the pressure coefficient behaviour changes dramatically.

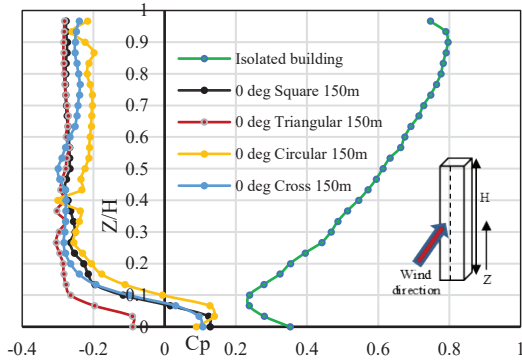


Figure 18 - C_p Variation with Building Height in Windward Face of Principal Building: 150 m 0- deg Case

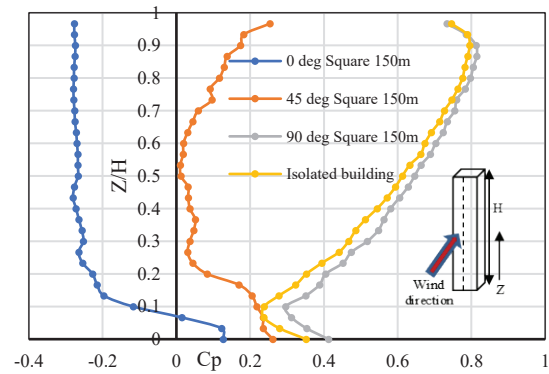


Figure 19 - C_p Variation with Building Height in Windward Face of Principal Building: 150 m Square

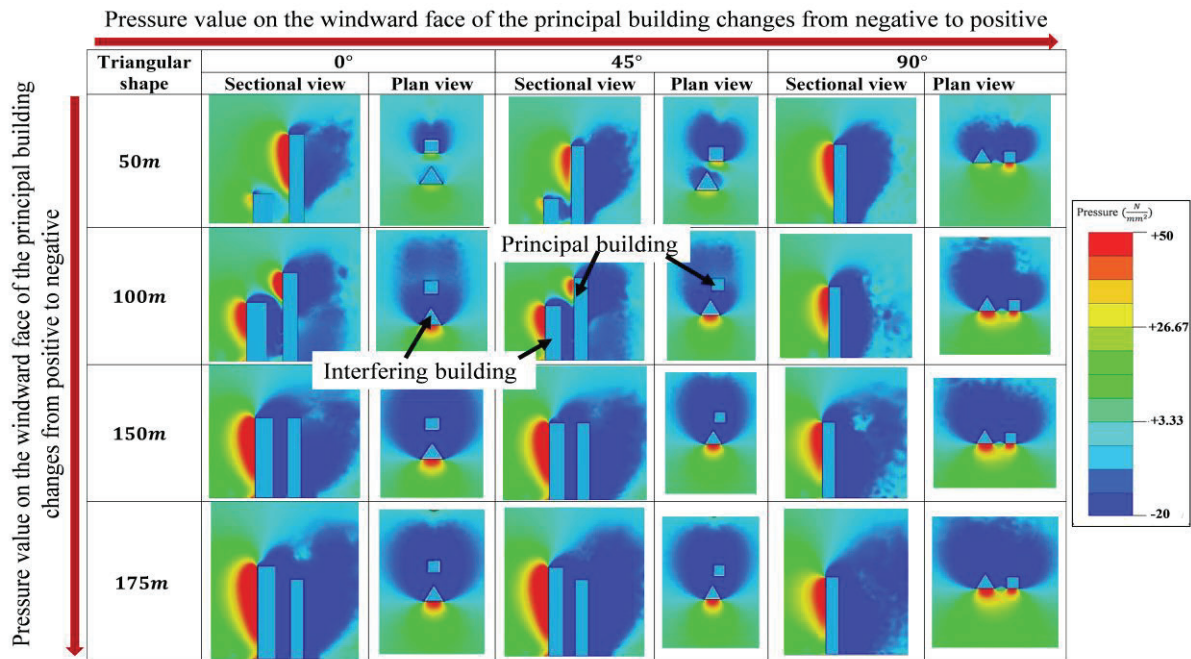


Figure 20 - Pressure Variations for Triangular Shape Interfering with Building with Different Angles and Height

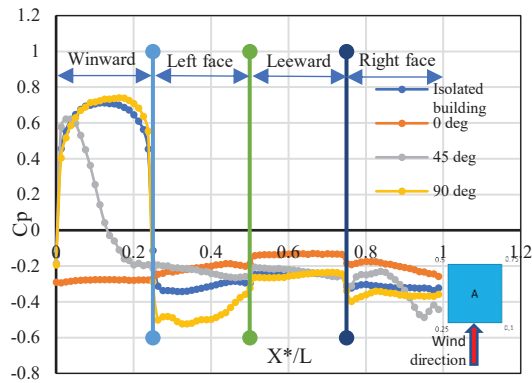


Figure 21 - Pressure Variation around the Principal Building at the 2/3 Height: 150 m Square Shape Cases

Figure 22 shows the pressure variation around the principal building at 2/3 height for 0-deg 150 m cases. The windward face is positive and the leeward and sidewalls are negative for the isolated model. However, a building interfered with an isolated model, and the behaviour of pressure coefficients is changing drastically. Based on the results, the maximum pressure variations for windward face, left face, leeward face and right face are for triangular, circular, cross, and circular shape, respectively.

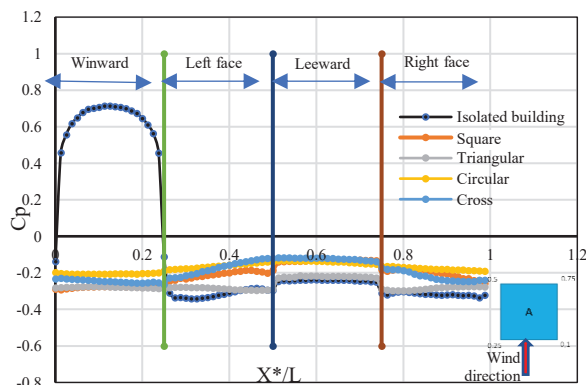


Figure 22 - Pressure Variation around the Principal Building at the 2/3 Height for 0-deg 150 m Cases

5. Conclusions

In this research, Computational Fluid Dynamics (CFD) was used to qualitatively and quantitatively study the effect of an upstream building configuration on a downstream building. From the several turbulence models available in the RANS approach, 0 equation model, 1 - equation $k - \epsilon$ model, 2 - equation Standard $k - \epsilon$ model, 2 - equation $k - \omega$ model, and 2 - equation $k - \omega SST$ model were compared to predict the pressure variations

around the building. From those models, the $2k - \omega SST$ model shows the least error ($MAPD$, MAD and MSD). It can be concluded that the $2k - \omega SST$ model is the most reliable turbulence model for this study. After validating and selecting the best turbulence model from the above models, the CFD analysis was performed to identify the interference effect on a square principal building from the upstream building with different shapes, namely, square, circular, cross, and triangular, with different orientations and heights. This study looked at the base moment, base shear, and pressure fluctuation of the principal building to assess the impact of the upstream building considering the interfering effects.

Based on the results, the maximum increments of the base moment and base shear in the triangular 90-deg and 175 m case were observed, and they were 32.38% and 31.30%, respectively. The results suggest that a safety factor for interfering effects should be considered in designing the building structures in the city area to ensure the stability of a building. And the maximum C_p variation in the triangular shape case was observed, and it was positive 0.8 to negative 0.3. The findings emphasized the significance of designing the cladding system's connection to both compression and tension forces. The results of the present study will be crucial in ensuring the stability and safety of the building structures when those buildings are going to be developed in a dense building environment.

For a particular orientation of the upstream building, the interference effects may change with the distance between the principal building and the interfering building. Also, it is recommended to consider the height of buildings beyond 200 m; this study is focused on the building height less than 200 m. Further, if there is a chance to conduct analysis by using LES or DNS other than RANS as a numerical method, it may give a more accurate prediction flow around the objects.

References

1. Kim, W., Tamura, Y., Yoshida, A. and Yi, J.H., "Interference Effects of an Adjacent Tall Building with Various Sizes on Local Wind Forces Acting on a Tall Building", *Advances in Structural Engineering*, Vol. 21, No.10, 2018, pp.1469-1481.
2. Chauhan, B.S. and Ahuja, A.K., "Height Effect of Interfering Buildings on Wind Pressure Distribution on Rectangular Plan Tall Buildings", In *9th Asia Pacific Conference Wind Engineering APCWE*, December, 2017, pp. 3-6.



3. Lo, Y.L., Kim, Y.C. and Li, Y.C., "Downstream Interference Effect of High-Rise Buildings Under Turbulent Boundary Layer Flow", *Journal of Wind Engineering and Industrial Aerodynamics*, 159, 2016, pp.19-35.
4. Quan, Y., Chen, J. and Gu, M., "Aerodynamic Interference Effects of a Proposed Taller High-Rise Building on Wind Pressures on Existing Tall Buildings", *The Structural Design of Tall and Special Buildings*, Vol. 29, No. 4, 2020, pp.1703.
5. Roy, A.K., Sardalia, A. and Singh, J., "Wind Induced Pressure Variation on High-Rise Geometrically Modified Building Having Interference Through CFD Simulation", *Computational Engineering and Physical Modeling*, Vol. 4(4), 2021, pp.26-38.
6. Li, Q., Zou, J., & Lu, L., "Interference Effects of the Height Changes of the Interfering Building on Wind Environment around a Tall Building", *Journal of Wind Engineering and Industrial Aerodynamics*, 174, 2018, pp.98-110.
7. Kiriparan, B., Jayasinghe, J.A.S.C. and Dissanayake, U.I., "Comparative Study of the Wind Codes: An Application to Forty-Six Storied Wall-Frame Structure", 2022.
8. Melbourne, W.H., "Comparison of Measurements on the CAARC Standard Tall Building Model in Simulated Model Wind Flows", *Journal of Wind Engineering and Industrial Aerodynamics*, Vol. 6, No.1-2, 1980, pp.73-88.
9. Szolomicki, J. and Golasz-Szolomicka, H., "Technological Advances and Trends in Modern High-Rise Buildings. *Buildings*", Vol. 9, No. 9, 2019, p.193.
10. Jafari, M. and Alipour, A., "Methodologies to Mitigate Wind-Induced Vibration of Tall Buildings: A State-of-the-Art Review", *Journal of Building Engineering*, Vol. 33, 2021, p.101582.
11. Vikram, M.B., Chandradhara, G. and Keerthi Gowda, B., "A Study on Effect of Wind on the Static and Dynamic Analysis", *International Journal of Emerging Trends in Engineering and Development*, Vol. 3, No. 6, 2014, pp.885-890.
12. Kiriparan, B., Jayasinghe, J.A.S.C. and Dissanayake, U.I., "Prediction of across Wind Response of Tall Buildings", An overview. In *ICSECM 2019: Proceedings of the 10th International Conference on Structural Engineering and Construction Management* Springer Singapore, 2021, pp. 383-397.
13. Holmes, J.D., "Dynamic Response of Structures to Wind Loading: Single- and Multiple Degree-of-Freedom Systems", *Journal of Wind Engineering and Industrial Aerodynamics*, 1994, 54-55, pp. 783-793.
14. Rima, T., "Wind-Induced Building Response: Effects of Wind Direction on Pressure Variations", *Journal of Wind Engineering and Industrial Aerodynamics*, 2019, 187, 45-56.
15. Mendis, P., Ngo, T., Haritos, N., Hira, A., Samali, B. and Cheung, J., "Wind Loading on Tall Buildings", *Electronic Journal of Structural Engineering*, 2007.
16. Cheung, J.C.K., & Melbourne, W.H. "A Review of Wind-Induced Response of Tall Buildings", *Journal of Wind Engineering and Industrial Aerodynamics*, 1992, 41-44, 1467-1476.
17. Lythe, G.M., & Surry, D. "Wind Loads on Tall Buildings: A Review", *Journal of Wind Engineering and Industrial Aerodynamics*, 1990, Vol. 34, No. 1-3, 235-242.
18. Isyumov, N., & Poole, A.B. "Wind Induced Response of Tall Buildings: Design Aids and Research Needs", *Journal of Wind Engineering and Industrial Aerodynamics*, 1983, Vol. 14, No. 1-3, 73-82.
19. Kareem, A. "Response of Tall Buildings to Wind Loads: A Critical Review", *Journal of Wind Engineering and Industrial Aerodynamics*, 1985, Vol. 20, No. 1-3, 15-40.
20. Tallin, A.G., & Ellingwood, B.R. "Wind Effects on Tall Buildings", *Journal of Structural Engineering*, 1985, Vol. 111, No. 2, 264-281.
21. Franek, M. and Macák, M., "Effects of Interference on Local Peak Pressures Between Two Buildings With an Elliptical Cross-Section", *Slovak Journal of Civil Engineering*, 2021, Vol. 29, No. 1, pp.35-41.
22. Saunders, C.C., & Melbourne, W.H. "Wind Loads on Tall Buildings", *Journal of the Structural Division*, 1979, Vol. 105, No. 12, 2441-2457.
23. Johnson, T. "A Comparative Study of RANS, LES, and DNS Methods in Computational Fluid Dynamics", *Journal of Engineering Applications*, 2019, Vol. 14, No. 3, 45-56.
24. Wang, S., Li, X., & Zhang, H. "Numerical Prediction of Mean Wind Loads on Buildings Using Reynolds-Averaged Navier Stokes

- Approach", *Journal of Wind Engineering and Industrial Aerodynamics*, 2018, 179, 52-65.
25. Dagnew, A.K. and Bitsuamlak, G.T., "Computational Evaluation of Wind Loads on a Standard Tall Building Using LES", *Wind and Structures*, 2014, Vol. 18, No. 25, pp.567-598.
 26. Murakami, S., "Overview of Turbulence Models Applied in CWE-1997", *Journal of Wind Engineering and Industrial Aerodynamics*, 1998, Vol. 74, pp.1-24.
 27. Tominaga, Y., Mochida, A., Yoshie, R., Kataoka, H., Nozu, T., Yoshikawa, M. and Shirasawa, T., 2008. "AIJ Guidelines for Practical Applications of CFD to Pedestrian Wind Environment around Buildings", *Journal of wind engineering and industrial aerodynamics*, Vol. 96. No. 10-11, pp.1749-1761.
 28. Huang, S., Li, Q.S. and Xu, S., "Numerical Evaluation of Wind Effects on a Tall Steel Building by CFD", *Journal of constructional steel research*, 2007, Vol. 63, No. 5, pp.612-627.
 29. Huang, S.H., Li, Q.S. and Wu, J.R., "A General Inflow Turbulence Generator for Large Eddy Simulation", *Journal of Wind Engineering and Industrial Aerodynamics*, 2010, Vol. 98, No.10-11, pp.600-617.
 30. Jayathilake R.G.S.N., Wijesundara K.K., "Prediction of Wind Induced Response of Tall Buildings using RANS Simulations", *IESL Annual Conference - The Institution of Engineers Sri Lanka*, Vol. 114, 2020.
 31. Weerasuriya A. U., "Computational Fluid Dynamic (CFD) Simulation of Flow around Tall Buildings", *ENGINEER - Vol. XXXXVI*, No. 03, 2013, 43-54
 32. Meng, F.Q., He, B.J., Zhu, J., Zhao, D.X., Darko, A. and Zhao, Z.Q., "Sensitivity Analysis of Wind Pressure Coefficients on CAARC Standard Tall Buildings in CFD Simulations", *Journal of Building Engineering*, 16, 2018, pp.146-158.
 33. Lin, C., & Chen, J. "Comparison of Wind Tunnel and Computational Fluid Dynamics Simulations for Wind-Induced Vibration Analysis of High-Rise Buildings", *Journal of Wind Engineering and Industrial Aerodynamics*, 2020, 196, 104-117.
 34. Chen, L. and Letchford, C.W., "Parametric Study on the Along-Wind Response of the CAARC Building to Downbursts in the Time Domain", *Journal of wind engineering and industrial aerodynamics*, Vol. 92, No. 9, 2004, pp.703-724.
 35. Mansouri, I., Chattopadhyay, A., & Kareem, A. "Effects of Plan Shape on Wind Loads and Responses of Tall Buildings", *Engineering Structures*, 2016, 122, 117-128.
 36. Kumar, A., & Sangle, S. "Wind Load Analysis on Tall Buildings of Different Plan Shapes", *International Journal of Engineering Research and Technology*, 2021, Vol. 14, No. 3, 1335-1342.
 37. Toronto city council, Tall Building Design Guidelines, City of Toronto, 2013. [online], <https://www.toronto.ca/wp-content/uploads/2018/01/96ea-cityplanning-tall-buildings-may2013-final-AODA.pdf>, Accessed: June 2022.

